Energy Efficiency Analysis for 802.15.6 based IR-UWB Body Area Wireless Sensor Networks

Irfan Ahmed

College of Computers and Information Technology
Wireless Communications and Networking Research Center,
Taif University, P.O.Box 888, Taif, Saudi Arabia
Email: i.ahmed@tu.edu.sa

Abstract—**This paper presents energy performance analysis of recently proposed IEEE 802.15.6 body area wireless network standard. This standard has provided specifications for four possible communication links in body area network. This paper focuses on the body surface to body surface channel (CM3) and body surface to external node channel (CM4). We provide analytical expressions for bit error rate and outage probability for impulse response ultra wide band (IR-UWB) using differential binary phase shift keying (DBPSK) modulation. Energy consumption per bit for CM3 and CM4 channels have been calculated for desired bit error rate in different channel conditions. Simulation results show that CM3 is more energy efficient and has low BER and as compared to CM4 for the same received SNR values and it is more susceptible to Rician factor due to the varying LOS/NLOS components.**

Keywords- body area sensor networks, energy efficiency, UWB.

I. Introduction

Body Area Network is a mix of sensor network technology and biomedical engineering. Professor Guang-Zhong Yang, first defined the phrase "Body Sensor Network" (BSN) with publication of his book Body Sensor Networks in 2006. BSN technology represents the lower bound of power and bandwidth from the BAN use case scenarios. Whereas, BAN technology has many potential uses in addition to BSNs. Some common use cases for BAN technology are: Body Sensor Networks (BSN),Sports and Fitness Monitoring, Wireless Audio, Mobile Device Integration, and Personal Video Devices etc. Each has unique requirements in terms of bandwidth, power usage, latency, and signal distance. Wireless Personal Area Networks (WPAN) has the working group with standard IEEE 802.15 which established a task group 6 to develop standards for BAN. The BAN task group has drafted a standard that covers a large range of possible devices. Using the standard, the developers can decide on how to balance data rate and power. Although the most obvious applications of BAN is the medical sector, there are more recreational uses to BAN. By this convenient means, patients and elderly people can keep track of their health conditions without frequent visits to the doctors offices. And the doctors can still, have access to the patients data and advise the patients accordingly.

Sensors have been long used in medicine and public health [1],[2]. They are embedded in variety of medical instruments for use at hospitals, clinics, and homes, sensors provide physiological and physical health states that are critical to the detection, diagnosis, treatment and management of ailments to patients and their health care providers. Driven by modern and advancing technology, medical sensors have become increasingly interconnected with other devices. They are capable of interfacing to external devices via wired interfaces such as RS232, USB and Ethernet. More recently they have incorporated wireless connections, both short range, such as Bluetooth, Zigbee and near field radios to communicate wirelessly to nearby computers, personal digital assistants, or smartphones, and long range such as WiFi or cellular communications to communicate directly with cloud computing services. With such wireless connections possible sensor measurements can be sent to the caregivers while the patients go through their daily work life away at home thus practicing real-time medical sensing.

IEEE 802 has established a task group called IEEE 802.15.6 for the standardization of WBAN. This serves as a communication standard optimized for low power in-body/on-body nodes for variety of medical and non-medical applications. This standard defines Medium Access Control (MAC) layer supporting several Physical (PHY) layers.

II. System, Signal and Channel Model

A. System Model

In the system model we use two body sensor nodes (source node is called relayed node and helping node is called relaying node) and one external or hub node as proposed in IEEE 802.15.6 two hop extension [3]. We assume that the selection of relaying node has already been made, e.g., the relayed node may select a node X as its relaying node if it recently received acknowledge frames sent from node X to the external node. The external node is a node that is not in contact with human body and it has a distance from human body in the range of few centimeters to up to 5 meters [4]. The system model in shown in Fig. 1.

In order to consider the total energy consumption, all signal processing blocks at the transmitter and the receiver need to be incorporated in the model. We consider the energy consumption in the building blocks of the RF front-end of differentially encoded DPSK transceiver. The transmitter and receiver RF front-ends are shown in Fig. 2 and 3, respectively. We have neglected the energy consumption in the baseband

circuit (i.e., source coding, pulse shaping, and digital modulation) because the power consumption in the baseband is mainly defined by the symbol rate and the complexity of the digital logic. This power consumption is quite small [5] compared with the power consumption in the RF circuitry.
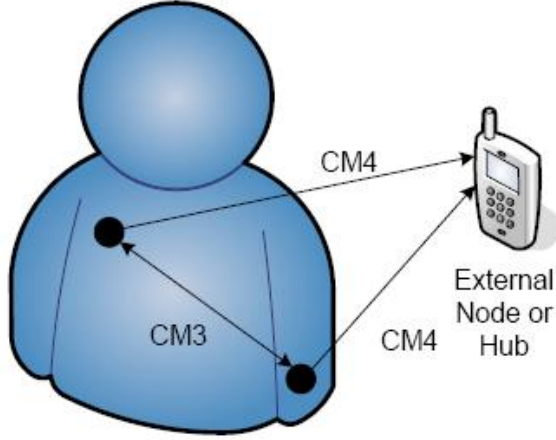
Figure 1: System Model
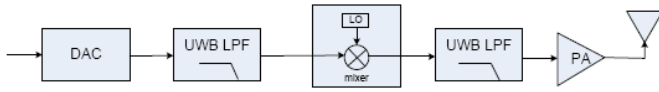
Figure 2: RF front-end for IR-UWB transmitter
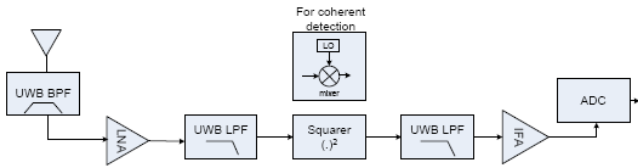
Figure 3: RF front-end for non-coherent IR-UWB receiver

B. Signal Model

We model the transmit signal as

$$s(t) = \Re\left\{ m(t)e^{j2\pi f_c t} \right\} \tag{1}$$

where $m(t)=x(t)+jy(t)$ is a complex baseband signal with bandwidth B, power P_m and for i^{th} differentially encoded BPSK or QPSK, it is given by $m_i(t)=m_{i-1}\exp(j\Theta_i)$. The power in transmitted signal $s(t)$ is $P_t=P_m/2$. The corresponding receive signal is the sum of line-of-sight (LOS) path and all resolvable multipath components:

$$r(t)=R\left\{ \sum_{n=0}^{N(t)} \alpha_n(t)m(t-\tau_n(t))e^{j(2\pi f_c(t-\tau_n(t))+\phi_{D_n})} \right\} \tag{2}$$

where $N(t)$ is the number of resolvable multipath components, ϕ_{D_n} is Doppler phase shift, α_n is the amplitude of receive signal, and $\tau_n(t)$ is n^{th} path delay with path length $r_n(t)$ such that $\tau_n(t)=r_n(t)/c$, (c is the velocity of light).

We rearrange the phase of received signal as

$$\phi_n(t)=2\pi f_c \tau_n(t)-\phi_{D_n} \tag{3}$$

Then the received signal is given by

$$r(t)=R\left\{ \left(\sum_{n=0}^{N(t)} \alpha_n(t)m(t-\tau_n(t))e^{-j\phi_n(t)} \right)e^{j2\pi f_c t} \right\} \tag{4}$$

C. UWB Channel Model

In this paper, we choose IR-UWB and use the channel model of the frequency band 3.1−10.6GHz [4]. In the body area network communications, propagation paths can experience fading due to different reasons, such as energy absorption, reflection, diffraction, shadowing by body, and body posture. As shown in Fig. 1, there are two types of channel models (CMs) corresponding to two different transmission links: the body surface to body surface link (CM3) and the body surface to external node link (CM4).

a) Body Surface to Body Surface CM3

Let d_{bb} denote the distance between two body sensor nodes in millimeter (mm). According to the body surface to body surface channel model [**Error! Reference source not found.**], the path loss model is given by

$$PL(d_{bb})[dB]=10log_{10}K+10log_{10}(d_{bb})^\gamma+\psi_{dB} \tag{5}$$

where K and γ are constants, and ψ_{dB} is normal random variable with zero mean and standard deviation σ_ψ. The time-varying impulse response $h(\tau,t)$ of this link, to impulse at $t-\tau$ is given by

$$h(\tau,t)=\sum_{n=1}^{N}\alpha_n(t)e^{-j\phi_n(t)}\delta(t-\tau_n(t)) \tag{6}$$

where α_n, τ_n, and ϕ_n denote the path amplitude, path delay, and phase for the *n-th* path, respectively. N is the number of the delay paths, and δ is the Dirac function. The phase φ_n is modeled by uniform distribution over $[0,2\pi)$. The path amplitude α_n is modeled by

$$10log_{10}|\alpha_n|^2 = \begin{cases} 0 & n=0 \\ \gamma_0 + 10log_{10}\left(\exp\left(-\frac{\tau_n}{\Gamma}\right)\right) + S & n\neq0 \end{cases}$$

$$(7)$$

where γ_0 is a Rician factor and Γ is a decaying factor with Rician factor, S is a normal distribution with zero-mean and standard deviation of σ_S. The random arrival time of multipath components with arrival rate λ is modeled by Poisson distribution as follow:

$$f(\tau_n|\tau_{n-1}) = \lambda\exp(-\lambda(\tau_n - \tau_{n-1})) \qquad (8)$$

Finally, the probability of N number of multipath components is given by

$$p(N) = \frac{\overline{N}^N\exp(\overline{N})}{N!} \qquad (9)$$

where $\overline{N}$ is the average number of the multipaths.

b) Body Surface to External CM4

The impulse response of a wireless channel between body sensor node and external node is given by

$$h(\tau,t) = \Sigma_{n=0}^{M-1}\beta_n(t)\delta(t-\tau_n(t)) \qquad (10)$$

here M is the number of arrival paths, modeled as Poisson random variable with mean $\overline{M}$, τ_n is the timing of arrival paths, modeled as Poisson random process with arrival rate λ, and β_n is the amplitude for the *n-th* path, given by

$$|\beta_n|^2 = \Omega_0\exp\left(-\frac{\tau_n}{\Gamma} - k[1-\delta(n)]\right)\zeta \qquad (11)$$

where Ω_0 is pathloss in free space, k is NLOS effect of Rician factor, $\zeta\sim lognormal(0,\sigma_\zeta)$, and $\tau_0 = d/c$ (d=TX-RX distance and c is the velocity of light). The path loss Ω_0 depends on the environment and line-of-sight situation. In the WBASN channel model report [**Error! Reference source not found.**, sec. 3.4], the value of Ω_0 is calculated for the four different angles between body surface node and external node. For zero degree angle, Ω_0 is given by

$$\Omega_0[dB] = 10log_{10}K + 10log_{10}(d_{be})^\gamma + y_{dB} \qquad (12)$$

where d_{be} is the distance between body surface node and external node and y_{dB} is the average received signal power at $t=\tau_1$. The specific values of all the parameters in these two types of channels can be found in [**Error! Reference source not found.**].

III. PROBLEM FORMULATION

A. Bit Error Rate Regime

Channel model CM3 has been proposed in IEEE 802.15.6 standard for this type of communication link. The channel gain $\alpha_n(t)$ between transmitter and the receiver is given by equation (7). In addition, the path loss and shadowing are modeled as power falloff proportional to the distance and lognormal random variable, respectively, as shown in equation (**Error! Reference source not found.**). In other words, on the top of path loss and shadowing, the signal is further attenuated by fading coefficient that depends upon Rician factor (γ_0), decaying factor (Γ), and a random variable (S) with normal distribution $S\sim(0,\sigma_S)$, given in equation (7). Let N be the actual number of resolvable multipaths in an impulse period 0 to t. These multipath components are resolvable in wideband and can be combined at the receiver using maximal ratio combining techniques [**Error! Reference source not found.**]. $\pi/2$ differential binary phase shift keying (DBPSK) is adopted as the modulation format. The instantaneous received SNR is given by

$$\gamma_b = ||\boldsymbol{\alpha}||_F^2\frac{E_b}{N_0} \qquad (13)$$

The received power of the N resolvable paths is estimated by using the power delay profile in equation (7)

$$||\boldsymbol{\alpha}||_F^2 = \sum_{n=1}^{N}10^{\frac{\gamma_0 + 10log_{10}\left(\exp\left(-\frac{\tau_n}{\Gamma}\right)\right)+S}{10}} \qquad (14)$$

The instantaneous bit error rate (BER) of DBPSK modulation in additive white gaussian noise (AWGN) channel is given by [**Error! Reference source not found.**]

$$P_b = \frac{1}{2}e^{-||\alpha_n||_F^2\frac{E_b}{N_0}} \qquad (15)$$

The probability density function (pdf) of the channel coefficient (α_n^2) can be determined by using function of random variables method [**Error! Reference source not found.**] and joint probability function of the product of two random variables [**Error! Reference source not found.**]. Given the pdf $f(x,y)$ of two random variables X and Y, the PDF of $V=XY$ is given by

$$f_V(v) = \int_{-\infty}^{\infty}f_{X,Y}\left(x,\frac{v}{x}\right)\frac{1}{|x|}dx \qquad (16)$$

Let $G_n = |\alpha_n|^2$, then (7) can be written as

$$G_n = \gamma_0' \exp\left(-\frac{\tau_n}{\Gamma}\right) S' \quad for \quad n \neq 0 \qquad (17)$$

Let $X = \exp(-\frac{\tau_n}{\Gamma})$ and $Y = \gamma_0' S'$, where τ_n has poisson distribution and S' has log-normal distribution. Using function of random variable method, we get the joint PDF $f(x,y)$ as

$$f(x,y) = \lambda e^{\lambda \Gamma ln|x|} \frac{1}{y\sigma\sqrt{2\pi}} e^{-\frac{\left(ln|y/\gamma_0'|\right)^2}{2\sigma^2}} \qquad (18)$$

Then, the pdf of G_n is given by

$$f(G_n) = \int_{x=1}^{0} \frac{\lambda}{\sigma\sqrt{2\pi}} e^{(\lambda\Gamma+1)ln|x| - \left(ln|G_n/x\gamma_0'|\right)^2 /2\sigma^2} dx \qquad (19)$$

Evaluation of this integral is intractable, therefore we adopt an alternative way. Equation (17) can be re-written for average value of channel gain as

$$\bar{G}(t) = \mathbf{E}\left[\sum_{n=0}^{N(t)-1} G_n \right] \qquad (20)$$

Decomposing the above expression for LOS and NLOS components:

$$\bar{G}(t) = \mathbf{E}\left[G_0 + \sum_{n=1}^{N(t)-1} G_n \right] \qquad (21)$$

Assuming the delay associated with LOS component is approximately equal to zero, then the PDF of the delay of the second arrival τ_1 is given by (8)

$$f(\tau_1) = \lambda e^{-\lambda \tau_1} \qquad (22)$$

From (21), the first term is a function of random variable S with zero mean and variance σ_S^2, therefore $\mathbf{E}_S[G_0] = \gamma_0' \exp\left(-\frac{\tau_1}{\Gamma}\right)$. With the substitution of this term, equation (21) becomes

$$\bar{G}(t) = \int_{\tau_1}^{t} [\gamma_0' e^{\left(-\frac{\tau_1}{\Gamma}\right)} + \bar{G}(t-\tau_1)]\lambda e^{-\lambda\tau_1} d\tau_1 \qquad (23)$$

Substituting $K_1 = \gamma_0'\lambda$ and $K_2 = \frac{1}{\Gamma} + \lambda$ in above integral, we get

$$\bar{G}(t) = \int_{\tau_1}^{t} [K_1 e^{-K_2\tau_1} + \bar{G}(t-\tau_1)\lambda e^{-\lambda\tau_1}]d\tau_1 \qquad (24)$$

The Laplace transform has applications throughout probability theory. We make use this transform to solve the above integral as

$$\bar{G}(Z) = \frac{1}{Z}\frac{K_1}{Z+K_2} + \frac{\lambda}{Z+\lambda}\bar{G}(Z) \qquad (25)$$

After some manipulation and taking inverse Laplace transform using Haeviside method, we get the following expression for the channel gain

$$\bar{G}(t) = \frac{K_1}{K_2^2}\left(K_2 - \lambda + (\lambda - K_2)e^{-K_2 t} + K_2\lambda t\right) \qquad (26)$$

The average SNR at the output of MRC receiver for a UWB pulse transmitted at $t=0$ is $\bar{\gamma}_b = \bar{G}(T)\frac{E_b}{N_0}$, where T is the period of UWB pulse. Hence, the BER is given by (15)

$$P_{b,CM3} = \frac{1}{2}\exp\left(-\bar{G}(T)\frac{E_b}{N_0}\right) \qquad (27)$$

and

$$P_{b,CM4} = \frac{1}{2}\exp\left(-\beta^2(T)\frac{E_b}{N_0}\right) \qquad (28)$$

where $\beta^2(T) = K_1' exp(-K_2'T) + \frac{\lambda K_1'}{K_2'}(1 - exp(-K_2'T))$ with $K_1' = \Omega_0\lambda exp(-k)$ and $K_2' = \frac{1}{\Gamma} + \lambda$.

B. Outage Probability

The outage probability relative to minimum required SNR ϑ_0 is defined as [**Error! Reference source not found.**]

$$P_{out} = p(\vartheta < \vartheta_0) = \int_0^{\vartheta_0} f_G(G) dG \qquad (29)$$

where $\vartheta = GE_b/N_0$ is the total SNR of the impulses at the receiver. In the UWB transmission, inverse of the signal bandwidth is smaller then the coherence time ($1/B << T_c$) therefore, a deep fade can affect many simultaneous symbols and fading may lead to large error bursts, which cannot be corrected for with coding of reasonable complexity. Therefore, these error bursts can seriously degrade end-to-end

performance. For UWB transmission, an outage probability is specified so that the channel is deemed unusable for some fraction of time or space. Channel gain in dB can be written as

$$G_{n,dB} = \begin{cases} K_{dB} + 10\gamma log_{10} d + \psi_{dB} & n=0 \\ \gamma_0 - \dfrac{10}{ln|10|\Gamma}\tau_n + Y + K_{dB} + 10\gamma log_{10} dn \neq 0 \end{cases} \quad (30)$$

where $Y = \psi_{dB} + S$ is a normal random variable with mean $\mu_\psi + \mu_S$ and variance $\sigma_\psi^2 + \sigma_S^2$ [**Error! Reference source not found.**, (2.1.104)]. Total channel gain for a UWB pulse transmitted at $t=0$ is given by

$$G_{dB}(t) = \|G_{n,dB}\|_F = G_0 + \sum_{n=1}^{N(t)-1} G_{n,dB} \quad (31)$$

Then the pdf $f(G)$ of the total instantaneous channel gain is obtained from the convolution of the pdfs of sum of N gamma random variable τ_n and the sum of N normal random variables Y. It has been proven that τ_n is a gamma random variable with parameters (n,λ) [**Error! Reference source not found.**]. The pdf of the sum of Gamma random variables is given by [**Error! Reference source not found.**, (2.9)]

$$f_\tau(t) = \dfrac{C \sum\limits_{k=0}^{\infty} \delta_k t^{\varrho+k-1} \lambda_{\varrho+k} e^{-\lambda t}}{\Gamma(\varrho+k)} \quad (32)$$

where ϱ, C, and δ are defined in [**Error! Reference source not found.**]. Using corollary 3 in [**Error! Reference source not found.**] with the condition that $\alpha_1 = 1, \alpha_2 = 2$ and so on, we get

$$f_\tau(t) = \dfrac{\lambda^{N(N+1)/2}}{\Gamma(N(N+1)/2)} t^{N(N+1)/2} e^{\lambda t} \quad (33)$$

Similar procedure for body surface to external node wireless channel CM4.

IV. ENERGY CONSUMPTION

A. Transmitter

A transmitter can be partitioned into three parts in terms of power/energy consumption. This partitioning is shown in Fig. **Error! Reference source not found.**. Power consumption in baseband part is proportional to the data rate. RF portion is responsible to upconvert the data to desired carrier frequency and therefore its power consumption depends on the RF frequency. Finally, the PA section is needed to transmit the information over the wireless medium. Its power consumption depends on its efficiency and on the required transmission range. Generally, RF block and PA are the most power hungry

parts in a transmitter. Transmitter power can be divided into three domains: i) transmission power P_{ON} i.e., the power required to transmit data over a distance d with desired BER, wake up power P_{WU} i.e., the power dissipated in RF block and PA during wake up period, and P_{SL} i.e., the power consumption in sleep mode.

$$P_{tx} = P_{ON,t} + P_{WU,t} + P_{SL,t} \quad (34)$$
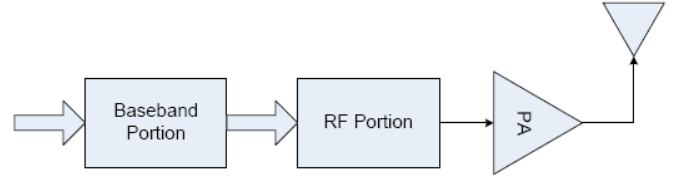
Figure 4: Transmitter power partitioning

The active mode power $P_{ON,t}$ consists of the transmission power and the circuit power consumption $P_{c,t}$ along the whole signal path.

$$P_{ON,t} = P_t + P_{PA} + P_{c,t} \quad (35)$$

where P_{PA} is the fraction of transmission power dissipated in power amplifier, and is given by $P_{PA} = \eta P_t$ with constant η which depends on the drain efficiency and peak-to-average power ratio of power amplifier [**Error! Reference source not found.**]. Substituting in (**Error! Reference source not found.**) and using above equation we get the following form

$$P_{ON,t} = (1+\eta) \dfrac{ln|2P_b|^{-1}}{\bar{G}(T)} N_0 R_b K d^l \psi + P_{c,t} \quad (36)$$

The second term $P_{c,t}$ is composed of power consumptions in digital to analog converter (DAC), UWB low pass filters (LPF), local oscillator (LO), and mixer. A typical low power $3.1-10.6 GHz$ transmitter using CMOS 65nm process consumed about 10.8mW from 1.2V source [**Error! Reference source not found.**].

B. Receiver

Low complexity UWB non-coherent receivers are very attractive for BAN applications because of very low power consumption (on the order of $10-100\mu W$), but the drawbacks are high noise and interference. A typical receiver RF section consists of a UWB bandpass filter (BPF), low noise amplifier (LNA), UWB LPF, a square law device, intermediate frequency amplifier (IFA), and analog-to-digital converter (ADC), as shown in Fig. **Error! Reference source not found.**. In case of coherent detection, the squarer is replaced by mixer and LO. A Low-Power CMOS RF front-end for non-coherent IR-UWB receiver consumed 17.5mA from 1.8V battery source [**Error! Reference source not found.**],

whereas, Verhelst et. al. [**Error! Reference source not found.**] have presented an IR-UWB coherent receiver which consumes 22.9mW with 1.8V supply. The choice of noncoherent versus coherent modulation is a key system-level tradeoff [**Error! Reference source not found.**]. Although coherent signaling schemes utilize bandwidth more efficiently and achieve better sensitivity than noncoherent schemes, for low-datarate systems these benefits come at the cost of degraded energy efficiency when normalized by data rate. This is due to the power cost of phase tracking hardware for coherent architectures. In this work, we have considered coherent receiver. Power consumption in receiver is given as

$$P_{rx}=P_{ON,r}+P_{WU,r}+P_{SL,r} \qquad (37)$$

The receiver ON state power is composed of; power consumption in receiver circuitry during data reception as well as the power consumption during listening the medium, i.e., $P_{ON,r}=P_{c,r}+P_{LS}$. The receiver circuit power consumption $P_{c,r}$ is given by the sum of power dissipations in UWB bandpass filter (BPF), UWB LPF, low noise amplifier (LNA), intermediate frequency amplifier (IFA), mixer, LO. and analog to digital converter (ADC).

V. SIMULATION RESULTS

In this section, we provide computer simulations using MATLAB. Bit error rate curves have been plotted against received SNR for CM3 and CM4 body area wireless channels. Values of constant parameters in CM3 and CM4 channels are given in table **Error! Reference source not found.** and table **Error! Reference source not found.**, respectively.

In Fig. **Error! Reference source not found.** BER performance of CM3 channel has been shown for different distances between body surface to body surface wireless nodes. For low values of E_b/N_0 there is a large error rate for all distances, but for the values greater than 20dB BER performance is abruptly improved, especially for shorter inter-node distances. Fig. **Error! Reference source not found.** shows the BER performance for CM4 channel. It can be seen that the performance improvement in CM4 is not comparable to CM3 because of changing LOS and NLOS components due to the random motion of human body. Also this channel has usually large inter-node distance causing more pathloss, shadowing, and fading. Fig. **Error! Reference source not found.** proves the effect of LOS/NLOS on BER performance. The total energy per bit has been evaluated in Fig. **Error! Reference source not found.** and Fig. **Error! Reference source not found.** for CM3 and CM4, respectively. Fig. **Error! Reference source not found.** shows that the effective energy per bit also increases exponentially with transmission rate R_b because increasing the bit rate, increases the number of MAC payload bits as well as the overhead bits, hence the energy consumption per payload bit is increased.

VI. CONCLUSIONS

Energy performance analysis of two commonly used wireless body area channel namely, CM3 and CM4, has been given in this paper. Analytical expressions for BER performance and channel gain probability distribution function with DBPSK modulation and IR-UWB transmission technology are derived. Energy consumption per bit for desired BER has been evaluated for CM3 and CM4. Simulation results depict that CM4 channel is more prone to BER because of the changing positions of human body. Results give the clue of using timely selective usage of two-hop extension (relay communications) to compensate the deep fade that can affect many simultaneous symbols and lead to large error bursts.
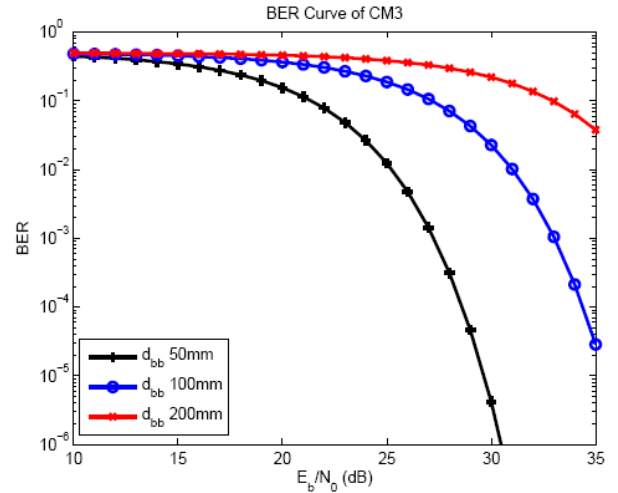
Figure 5: BER curve for CM3 channel
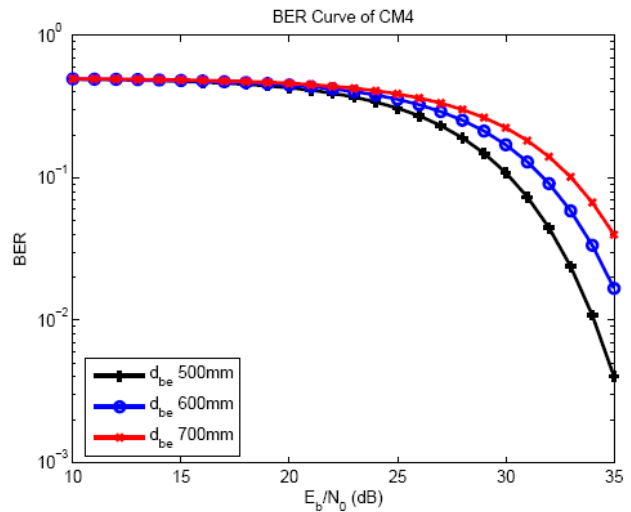
Figure 6: BER curve for CM4 channel
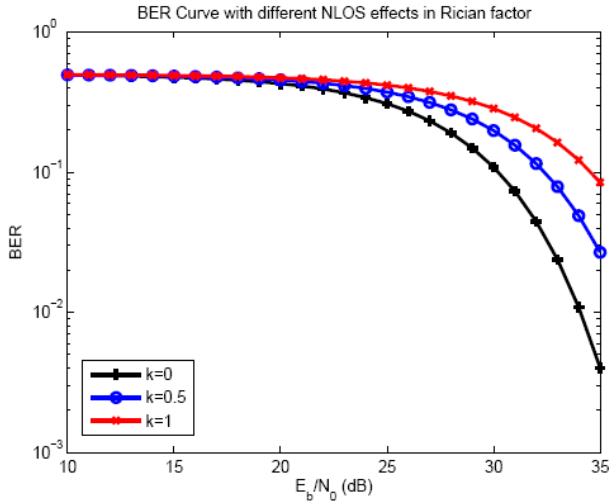
Figure 7: BER performance with different NLOS effects

Figure 8: Total energy consumption per bit in CM3

TABLE I
PARAMETER VALUES OF CM3

Characteristic	Parameter	Value
Pathloss	K	3.38 dB
	γ	1.92
	σ_ψ	4.40 dB
Power delay profile	γ_0	-4.60 dB
	Γ	59.7 ns
	σ_S	5.02 dB
	$1/\lambda$	1.85 ns
	$\overline{N}$	38.1

TABLE II
PARAMETER VALUES OF CM4

Characteristic	Parameter	Value
Pathloss	η_{dB}	22.2
Power delay profile	k	5.111
	$\overline{N}$	400
	$1/\lambda$	0.50125 ns
	Γ	44.6346 ns
	σ_ζ	7.30 dB
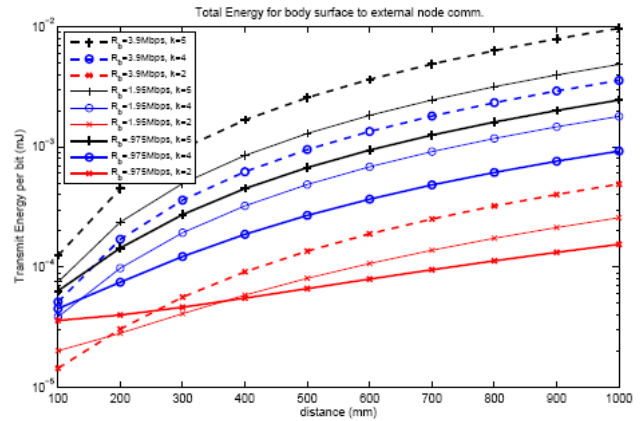
Figure 9: Total energy consumption per bit in CM4

REFERENCES

[1] P. Aberg, T. Togawa, and A. Spelman, *Sensors Applications Volume 3,Sensors in Medicine and Health Care*. plus 0.5em minus 0.4emwiley, 2002.

[2] C. Wilson, "Sensors in medicine," *Western Journal of Medicine*, vol. 171, no. 5-6, pp. 322–325, Nov-Dec 1999.

[3] "IEEE standard for local and metropolitan area networkspart 15.6: Wireless body area networks," *IEEE Std 802.15.6-2012*, pp. 1 –271, 29 2012.

[4] *Channel Model for Body Area Network (BAN)*, IEEE Std. IEEE P802.15-08-0780-09-006, 2009.

[5] S. Cui, A. Goldsmith, and A. Bahai, "Energy-constrained modulation optimization," *Wireless Communications, IEEE Transactions on*, vol. 4, no. 5, pp. 2349 – 2360, sept. 2005.

[6] T. Aoyagi, J. ichi Takada, K. Takizawa, H. Sawada, N. Katayama, K. Y. Yazdandoost, T. Kobayashi, H.-B. Li, and R. Kohno, *Channel models*

for wearable and implantable WBANs, IEEE Std. IEEE P802.15, Rev. 15-08-0416-03-0006, 2008. [Online]. Available: https://mentor.ieee.org/802.15/dcn/08/15-08-0416-03-0006-channel-models-for-wearable-and-implantable-wbans.doc

[7]	A. Goldsmith, *Wireless Communications*. plus 0.5em minus 0.4emUK: Oxford University Press, 2005.

[8]	T. Rappaport, *Wireless Communications Principles and Practice*. New Jersey: Prentice Hall, 1996.

[9]	J. G. Proakis, *Digital Communications*.New York, NY, 10020: McGraw-Hill, 2001.

[10]	J. Gray and S. Addison, "Characteristic functions in radar and sonar," in *System Theory, 2002. Proceedings of the Thirty-Fourth Southeastern Symposium on*, 2002, pp. 31 – 35.

[11]	H. Hsu, *Probabilty, Random Varables, and Random Processes*. York: McGraw Hill, 2010.

[12]	P. Moschopoulos, "The distribution of the sum of independent gamma random variables," *Annl. Inst. Statist. Math.*, vol. 37, pp. 541–544, 1984. [Online]. Available: http://www.math.utep.edu/Faculty/moschopoulos/Publications/

[13]	M. Akkouchi, "On the convolution of gamma distributions," *Soochow Journal of Mathematics*, vol. 31, no. 2, pp. 205–211, 2005.

[14]	P. Simitsakis, Y. Papananos, and E.-S. Kytonaki, "Design of a low voltage-low power 3.1-10.6 ghz uwb rf front-end in a cmos 65 nm technology," *Circuits and Systems II: Express Briefs, IEEE Transactions on*, vol. 57, no. 11, pp. 833 –837, nov. 2010.

[15]	Y. Gao, Y. Zheng, and C.-H. Heng, "Low-power CMOS RF front-end for non-coherent IR-UWB receiver," in *Solid-State Circuits Conference, 2008. ESSCIRC 2008. 34th European*, sept. 2008, pp. 386 –389.

[16]	M. Verhelst and W. Dehaene, "Analysis of the QAC IR-UWB receiver for low energy, low data-rate communication," *Circuits and Systems I: Regular Papers, IEEE Transactions on*, vol. 55, no. 8, pp. 2423 –2432, sept. 2008.

[17]	A. Chandrakasan, F. Lee, D. Wentzloff, V. Sze, B. Ginsburg, P. Mercier, D. Daly, and R. Blazquez, "Low-power impulse UWB architectures and circuits," *Proceedings of the IEEE*, vol. 97, no. 2, pp. 332 –352, feb. 2009.

AUTHORS PROFILE

Irfan Ahmed received the B.E. Electrical Engineering degree from University of Engineering and Technology, Taxila, Pakistan, in 1999, the M.S. Computer Engineering degree from CASE, Islamabad, Pakistan, in 2003, and the PhD degree in Telecommunication Engineering from Beijing University of Posts and Telecommunications, Beijing, China, in 2008.

He was post-doctoral fellow with Qatar University from April 2010 to March 2011, where he worked on, wireless mesh networks with Purdue University, USA, and radio resource allocation for LTE with Qtel. He has also been involved in National ICT Pakistan funded research project "design and development of MIMO and Cooperative MIMO test-bed" at Iqra University, Islamabad, Pakistan, during 2008 to 2010. His research interests include wireless LAN (WLAN) medium access control (MAC) protocol design and analysis, cooperative communications, performance analysis of wireless channels, energy constrained wireless networks, and radio resource allocation. He is an author of more than 20 International publications.